International Journal of Civil Engineering (2019) 17:333–346
https://doi.org/10.1007/s40999-017-0275-7

RESEARCH PAPER

Experimental Study on Seismic Performance of Ungrouted Confined Concrete Masonry Walls with Unbonded Tendons

Zhanggen Guo[1,2] · Songlin Zheng[1] · Zhenwen Xu[1] · Weimin Sun[1]

Received: 10 April 2017 / Revised: 24 October 2017 / Accepted: 2 December 2017 / Published online: 13 December 2017

Abstract

A novel concrete masonry wall for enhancing seismic behavior is adopted and justified in this paper, namely, ungrouted posttensioned confined concrete masonry (PTCCM) wall with unbonded tendons. The wall is posttensioned as well as confined by the ring beam placed on the top and constructional columns placed at the both ends of the wall. To validate the effectiveness of this technique, 14 walls were tested under lateral cyclic loads. The main parameters studied in this research are prestressing level, opening and horizontal reinforced concrete strip as well as axial load. The damage pattern and failure mode, force deformation response, ultimate strength, ductility and damping coefficient of each wall were carefully studied as well as stiffness degradation. The effects of posttensioning, opening and horizontal reinforced concrete strip on the seismic behavior of the PTCCM walls were analyzed in detail. The test results indicate that the posttensioning is significantly effective in improving the cracking resistance and seismic behavior, slowing down the stiffness degradation, as well as enhancing the shear and energy dissipation capacity of the PTCCM walls. The confinement effect provided by the ring beam and constructional columns can effectively improve the seismic behavior of the concrete masonry walls. By utilizing unbonded posttensioning, the ungrouted PTCCM walls had little residual deformation after cyclic loading. It can also be concluded that horizontal reinforced concrete strip can increase the cracking resistance, ductility and energy dissipation capacity of the walls. Based on the test results, a simple analysis method for predicting the shear strength of the PTCCM walls is proposed.

Keywords Concrete masonry · Posttensioning · Shear strength · Ungrouted · Seismic behavior

List of Symbols

A_c, h_0	The cross-section area and effective length of constructional columns (mm^2, mm)
A_m, f_v	The cross-section area and shear strength of masonry walls (mm^2, MPa)
A_{sv}, f_{yv}	The section areas and yield strength of stirrups (mm^2, MPa)
f_1, f_2	The average compressive strengths of concrete blocks and mortar (MPa)
f_m, f_{cu}	The average compressive strengths of masonry prisms and concrete (MPa)
f_{vo}	The average shear strength of masonry prisms in the absence of vertical compression stress (MPa)
P_c, P_u	The measured initial cracking strength and shear strength of test walls (KN)
s	The distance between stirrups (mm)
V_u	The predicted ultimate shear strength of test walls (KN)
V_m, V_c	The shear capacities provided by masonry walls and constructional columns (KN)

Zhanggen Guo and Songlin Zheng are equally contributed to this manuscript as co-first author.

✉ Zhanggen Guo
zhgguo@njtech.edu.cn; guoz5@uw.edu

Songlin Zheng
zhengslchn@163.com

Zhenwen Xu
1046228587@qq.com

Weimin Sun
swmdwg@njut.edu.cn

[1] College of Civil Engineering, Nanjing Tech University, No. 30 Puzhu Road(S), Nanjing 210009, China

[2] Present Address: Department of Civil and Environmental Engineering, University of Washington, Seattle 98195-2700, USA

σ_{s1}, σ_{s2}	The average yield strengths of PT tendons and longitudinal reinforcements (MPa)
σ_y	Total axial compression stress of test walls (MPa)
σ_p	Additional axial compression stress of test walls provided by posttensioning (MPa)
ζ_p	Effective coefficient to account for the contribution of PT tendons elongation in increasing the shear capacity of test walls (−)
ζ_g	Reduction coefficient to account for the insufficient development of the constructional columns (−)
ξ_e	The equivalent viscous damping coefficient of test walls (−)
$\Delta_c, \Delta_y, \Delta_u$	The cracking, equivalent yield and ultimate displacements of test walls (mm)
γ_u, μ	The ultimate drift capacity and displacement ductility factor of test walls (−)
α	Regression factor (−)
μ_o	The friction coefficient between mortar joints (−)

1 Introduction

For many decades, masonry has been used as a common structural material in a large proportion of buildings in China. Currently in China, approximately 95% of the residential houses in vast rural areas are masonry structure. Since 1990s, with problems of environmental pollution, lack of land resources and consumption of energy, fired common clay bricks have been forbidden to use in China. Concrete hollow blocks, possessing many advantages over traditional masonry materials, such as high strength and labor productivity, light weight, soil and energy saving, environmental friendly, have been widely used to build low-rise buildings in the last two decades [1]. However, limited critical crack resistance and shear capacity provided mainly by friction in mortar joints result in severe cracking under gravity and temperature loads as well as sliding and collapse under earthquake. A great number of unreinforced concrete block masonry buildings suffered severe damage or even collapsed in 2008 Wenchuan earthquake and 2010 Yushu earthquake in China [2]. As a result, improving the cracking resistance and seismic performance of concrete masonry walls is of great importance.

It has been well known that the shear and tensile strengths of the masonry are usually less 10% of its compressive strength. Furthermore, the shear strength of masonry increases with the vertical compressive strength increasing in a wide range [3, 4]. If an appropriate amount of vertical axial load provided by posttensioning is applied to the masonry walls, the posttensioning will reduce or eliminate tensile stress within the walls and subsequently increases the lateral force required to initiate cracking, thus enhances the cracking resistance and shear strength of the walls. These disadvantages above may be overcame [5].

In the last century, the vast majority of past research focused on posttensioned brick retaining walls and bridge decks as well as veneer elements [6]. Over the last 15 years, several researchers were interested in grouted posttensioned concrete masonry (PTCM) walls. Laursen and Ingham [7–9] conducted a series of test on seismic behavior of the PTCM walls and concluded that fully grouted PTCM wall is a competent material combination for ductile structural wall systems and reliable drift capacity beyond 1% is likely to be achieved. The lateral force–displacement response can be described by a nearly non-linear elastic relationship and there are no residual post-earthquake displacements. Rosenboom and Kowalsky [10] found reduced deformation capacity and quick loss of strength in the bonded posttensioned brick masonry walls under seismic loading. So bonded posttensioned bar was not recommended to use in posttensioned masonry walls, and it was suggested that the posttensioned bar should be designed to remain elastic to avoid regions of low stiffness after extensive loading. Wight and Kowalsky [11] conducted shake table test on PTCM walls with openings, validating the ability of PTCM walls to self-center. Wight and Ingham [12] designed and constructed a PTCM house in New Zealand, demonstrating that posttensioned wall system can be simply integrated into existing floor and foundation. Hassanli [13] recently found that PTCM walls having the same total initial posttensioning force but different stress levels in the posttensioned (PT) tendons displayed different shear strengths. Doubling the total initial posttensioning force in PT tendons can not significantly increase the shear strength of the walls. In addition, Hassanli [14] implemented parametric studies on PTCM walls using finite element method.

These above studies underline the large potential of using posttensioning in conjunction with concrete masonry walls because the material properties of concrete masonry are similar to those of concrete. The advantages of the grouted PTCM walls can be concluded as follows [7–10]: first, the PT tendons can be conveniently placed in the vertical holes inside the walls and the use of PT tendons as primary longitudinal reinforcement can substantially simplify the construction process. Second, posttensioning offers a restoring effect on masonry walls (i.e. PTCM walls are "self-corrects"). As long as the PT tendons retain a significant force, they will return the walls to their initial position. There is few residual displacement after excessive loading, thus yielding PTCM walls would require very little repair. Third, posttensioning can effectively strengthen connections between walls and diaphragms to avoid the failure of joints. Finally, the additional axial loads provided by posttensioning

increase the cracking resistance and shear capacity as well as simultaneously improve the seismic performance of the masonry walls.

Although the construction process of the ungrouted PTCM walls is much simpler compared to the grouted PTCM walls, Laursen and Ingham [9, 10] found that the ungrouted PTCM walls revealed limited ductility and drift capacity as well as poor seismic behavior. To improve the seismic performance of ungrouted PTCM walls, a novel ungrouted posttensioned confined concrete masonry (PTCCM) wall is proposed in this paper. Instead of grouting, concrete ring beam placed on the top and constructional columns placed at the both ends of the walls are adopted to confine the masonry walls. Constructional columns and ring beam are cast in place, after the construction of the walls. This kind of masonry wall is usually called confined masonry. It should be noted that the constructional columns and ring beam are structural measures and different from the structural members of frame structure.

A feasible method employing the PTCCM walls with unbonded tendons is shown in Fig. 1. The concrete masonry wall is constructed first, then the concrete constructional columns and ring beam are cast in place. With appropriate treatments against corrosion, the PT tendons are passed through the vertical ducts located inside the wall and remain unbonded. The lower end of the PT tendons can be rigidly anchored into the concrete foundations. The masonry wall is posttensioned by tensioning the upper end of the PT tendons with a hydraulic jack or torque wrench.

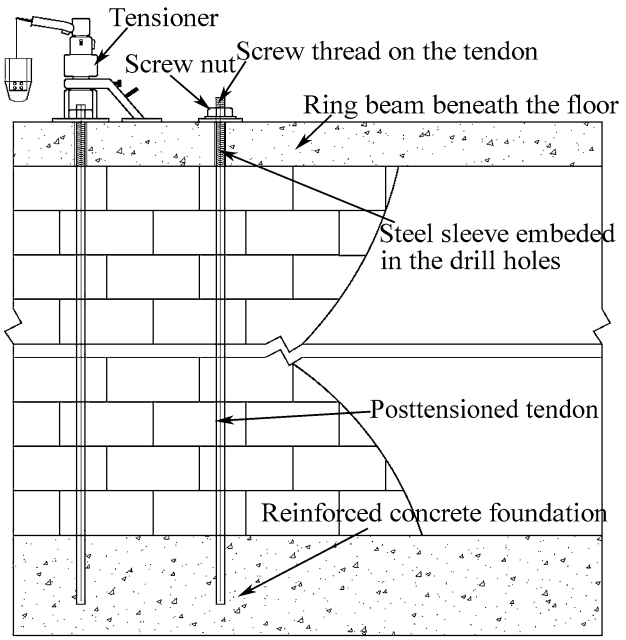

Fig. 1 Scheme of unbonded PTCCM walls

Compared to the grouted PTCM walls and reinforced concrete masonry walls, the advantages of the ungrouted PTCCM walls can be concluded as follows: (1) the vertical cells are not grouted so that the construction process of the ungrouted PTCCM walls is much simpler and the mass of the wall can be greatly declined, resulting in reduced inertia forces under seismic loading and gravity loads to the foundations of the buildings. (2) The concrete and steel bars are saved, thus the cost of the ungrouted PTCCM walls can be highly reduced.

2 Research Objective and Methods

The objective of this research is to verify the efficacy of the ungrouted PTCCM walls as a masonry structure system to build low-rise houses. To establish suitable seismic design criteria for PTCCM walls, 14 concrete masonry walls, including three companion control walls and 11 PTCCM walls, were tested under cyclic lateral loads and constant axial load. A complete description of the experimental results is presented, including assessment of test observations, strength, deformation and energy dissipation capacity as well as stiffness degradation. The effects of posttensioning, opening and horizontal reinforced concrete strip on the seismic behavior of PTCCM walls were carefully analyzed. Based on the test results, a simple approach for predicting the shear strength of PTCCM walls is proposed. This research presented herein is part of a larger research program, with the intention of developing a new concrete masonry structure for multi-storey residential construction and office buildings.

3 Experimental Programme

3.1 Test Specimens

A total of three series, 14 1:2 scaled masonry walls were designed according to Chinese National Standard [15], simulating various typical walls of low-rise concrete masonry buildings. The main parameters studied in this test are prestressing level, opening and horizontal reinforced concrete strip as well as axial load. The details of each wall are shown in Table 1. The geometric dimension and reinforcement details of the specimens as well as PT tendons layout are illustrated in Fig. 2. All masonry walls had the same length of 2.4 m, height of 1.8 m, thickness of 0.19 m, with aspect ratio being 0.75. The eight walls in series I included a control specimen (i.e., specimen W-1 without prestressing force), and seven posttensioned walls. The opening dimension is 800 mm × 800 mm. Specimens Yw-a and Yw-b are identical to other specimens, with the exception that horizontal

Table 1 Details of test specimens

Series no.	Specimen	Type of the wall	Axial stress (MPa)	Prestressing (MPa)	Load ratios	Typical walls of masonry building
1	W-1	Control wall	0	0	0	External longitudinal wall with opening
	Yw-1	Posttensioned wall with opening	0	0.38	0.133	
	Yw-2		0	0.47	0.165	
	Yw-3		0	0.43	0.151	
	Yw-4		0	0.50	0.175	
	Yw-5		0	0.40	0.067	
	Yw-a	Posttensioned wall with opening and horizontal concrete strip	0	0.378	0.064	
	Yw-b		0	0.463	0.078	
2	W-a	Control wall	0	0	0	Internal longitudinal wall without opening
	Yw-c	Posttensioned wall without opening	0	0.392	0.066	
	Yw-d		0	0.465	0.078	
3	Dw-1	Control wall	0.319	0	0.56	Internal cross wall
	DYw-1	Posttensioned wall applied axial stress	0.319	0.449	0.136	
	DYw-2		0.319	0.538	0.151	

reinforced concrete strip placed below the opening, which were designed to investigate the effectiveness of horizontal reinforced strip in improving the cracking resistance and seismic performance of masonry walls. In series I and III, three walls without opening were manufactured. W-a and Dw-1 are control specimen as well as Yw-c, Yw-d, DYw-1and DYw-2 are posttensioned walls. In series I and II, these walls were designed to model longitudinal walls and not applied axial load because longitudinal walls usually bear very few floor loads and live loads. Thus, the gravity was directly analogous to a component of the applied prestressing force (i.e. a part of the prestressing force was assumed to account for the gravity load). These walls in series III were designed to model internal cross walls and applied a constant axial compression stress of 0.319 MPa, replicating axial gravity and live loads from suspended floors.

All walls were constructed with standard precast concrete hollow block, which is primarily 390 mm in length, 190 mm in width and 190 mm in thickness. The vertical cells inside the wall were ungrouted. Constructional columns and ring beam were casted in place, after the construction of the walls. The columns and beams had the same dimension, which is 200 mm × 190 mm and were reinforced with four longitudinal reinforcements and transverse stirrups. The horizontal concrete strip had a cross section of 190 mm × 60 mm and was reinforced with longitudinal reinforcements and transverse stirrups. Bottom beam with a cross section of 450 mm × 300 mm connected with the wall, simulating solid boundary conditions.

All PTCCM walls were posttensioned with four PT tendons, which were placed in the vertical ducts located inside the wall to accommodate the masonry modular dimension, be symmetric, and provided an approximately uniform distribution of posttensioning to the walls, as shown in Fig. 2. The PT tendons used in this test are high-tensile thread bars with a nominal diameter of 18 mm. The walls were applied different prestressing forces, resulted in various axial compression ratio. The following posttensioning procedure was adopted. The PT tendons were first anchored into the foundations at the lower end and then were stretched by tightening the screw nuts using torque wrench, which is similar to torque control-method of high-strength bolts. After reaching a designed value of prestressing force, the screw nuts at the upper end of the PT tendons were tightened to fix the prestressing. The space between PT tendons and surrounding ducts was unfilled after the posttensioning was applied, as a result, the PT tendons were left unbonded. The prestress loss was measured for a period of 6 h, which is about 8% for ungrouted PTCCM walls. The possible prestress losses are the relaxation of prestressing tendons, masonry compression and anchorage loss. The prestress losses were effectively reduced by restressing the PT tendons just before the test.

3.2 Material Properties

Material properties tests on masonry and its constituents, concrete, PT tendons, longitudinal reinforcements and stirrups were carried out according to Chinese National Standard [16–18], typically in samples of five. These samples were constructed and subjected to the same curing condition as well as tested at the same time as the specimens. The average compressive strengths of concrete block f_1, mortar cubes f_2, masonry prisms f_m, concrete cubes f_{cu} and shear strength of masonry prisms f_{vo} as well as yield strengths of

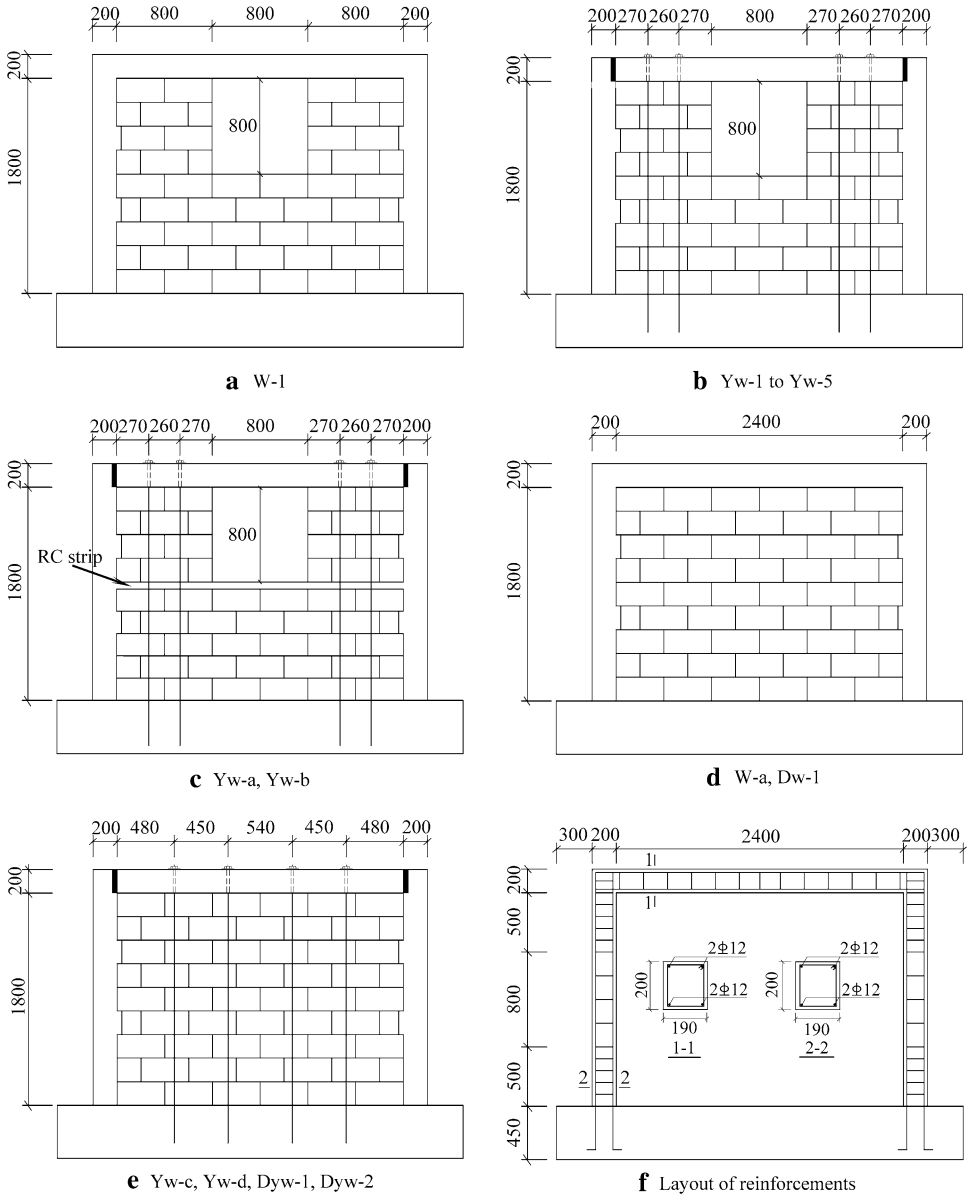

Fig. 2 Specimen details and layout of posttensioned (PT) tendons and reinforcements (all dimensions in mm)

PT tendons $\sigma_{s1}$and longitudinal reinforcements σ_{s2} are summarized in Table 2.

3.3 Experimental Set-up, Instrumentations and Load history

The experimental setup adopted is shown in Fig. 3. The concrete foundation was fixed to the ground floor using four 70 mm diameter steel rock bolts penetrating the foundation

Table 2 Average mechanical properties of materials

Specimen	Concrete block	Mortar	Masonry		Concrete	PT tendons	Reinforce-ments
	f_1 (MPa)	f_2 (MPa)	f_m (MPa)	f_{vo} (MPa)	f_{cu}(MPa)	σ_{s1} (MPa)	σ_{s2} (MPa)
W-1, YW-1 to YW-4	5.20	8.14	2.85	0.12	22.07	542	348
YW-5, W-a, YW-a to YW-d	13.51	10.02	5.95	0.17	22.98	542	348
DW-1,DYW-1, DYW-2	11.0	9.3	5.65	0.15	26.7	540	360

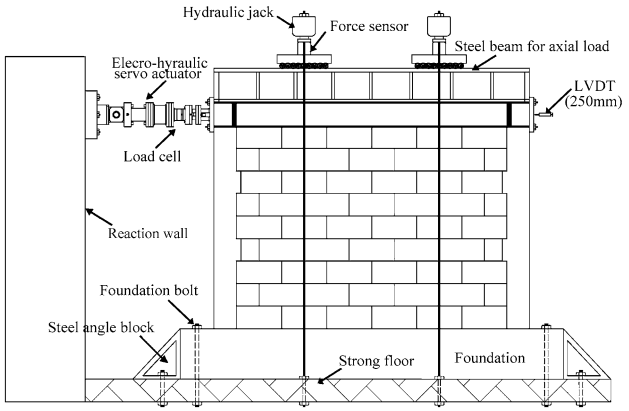

Fig. 3 Experimental set-up

and experimental pedestal, and two steel angle blocks on both ends of the foundation. Cyclic lateral loads were applied using an electro-hydraulic servo actuator. For these walls of series III, four hydraulic jacks were placed symmetrically on steel beam which were installed on the ring beam, and provided an approximately uniform distribution of axial load to the masonry walls, resulting in a designed axial compression stress of 0.319 MPa.

The cyclic lateral loads were recorded using a load cell attached to the hydraulic actuator. Lateral displacement at the application point of the lateral load were recorded using a linear variable displacement transducer (LVDT) which was placed on a steel tripod installed on the foundation for the modifications of the measured top deformations. Electrical resistance strain gauges were used to measure the strain of the PT tendons.

All masonry walls were subjected to cyclic lateral loads, which were controlled by the sequential displacement loading history. All specimens were cycled two times in each direction (push and pull excursion) at each displacement loading level. The test was terminated when the lateral load had degraded below 85% of maximum load, according to Chinese specification for seismic test method [19].

4 Test Results and Discussions

4.1 Damage Pattern and Failure Mode

Specimen W-1 is control wall with opening. At a drift ratio of 0.054% (0.98 mm), a fine crack formed in the horizontal mortar joint at the upper part between the opening and column. Cycling continued with this crack developed along the mortar joints, and further cracks were observed. Stepped-shape cracks gradually extended throughout the wall and formed X-shape cracks afterwards. At a drift ratio of 0.503% (9.06 mm), the maximum load of 85 kN was achieved, accompanied by the crushing of localised block, resulting in strength degradation. The test for specimen W-1 was terminated due to the severe sliding along the X-shape cracks. Specimens Yw-1 to Yw-5 are posttensioned walls with opening. At a deformation about 1.0 mm, first crack formed in vertical mortar joint at the toe region of the window, which is different from specimen W-1. The crack developed along the mortar joints and other cracks were observed during further loading. The PT tendons started to play a role after the occurrence of the cracks. Due to the restoring forces provided by the tendons, these cracks closed when walls were unloaded. Specimens Yw-a and Yw-b are posttensioned walls with horizontal concrete strip. The structural behavior of these walls is similar to that of the replicate posttensioned walls with the exception that the occurrence of first crack was delayed and fewer cracks with smaller width showed in the wall above the horizontal concrete strip.

W-a is control wall as well as Yw-c and Yw-d are posttensioned walls without opening. All of the specimens were mainly governed by shear deformation and exhibited cracks first along the horizontal mortar joints at a drift ratio of about 0.05%. For these posttensioned walls, the cracks closed and residual displacements are minimal when walls were unloaded. All specimens reached its ultimate capacity with the formation of the X-shape diagonal cracks and the occurrence of cracks along the constructional columns. By increasing the friction of the mortars, the posttensioned walls were able to sustain much higher lateral load. In addition, after the peak load, although the lateral deformation increased rapidly, the lateral load almost remained constant for these walls.

Dw-1 is control wall as well as DYw-1 and DYw-2 are posttensioned walls with a vertical compression stress of 0.319 MPa. The initial performance of these walls is similar and first crack formed in the horizontal mortar joint, regardless of the posttensioning. After the occurrence of the first crack, the lateral deformation increased rapidly, accompanied by the decrease of the stiffness. The ultimate shear capacity was achieved, after the cracks extended throughout the wall and into the constructional columns. The lateral displacement at the occurrence of the diagonal X-shape cracks was significantly larger in posttensioned walls DYw-1 and DYw-2 than in control wall Dw-1. The lateral load decreased gradually during further loading. Control specimen Dw-1 showed severe diagonal tension cracks passing through the mortars, while the width of the cracks in posttensioned walls DYw-1 and DYw-2 is significantly reduced.

All walls generally performed in a similar manner and clearly revealed shear dominated response, signified by development of X-shape diagonal shear cracks spanning across the wall, eventually leading to shear failure in both directions of loading. Due to the confinement effect provided by the ring beam and constructional columns, none of these

walls suffered from sudden failure. The cracking pattern of each wall is shown in Fig. 4. For these walls made with low strength block (i.e., yw-2, yw-3, yw-4), the failure occurred in the concrete blocks and some block face shell spalling were observed. For these walls made with high strength block, the cracks followed the vertical and horizontal mortar joints and no blocks were crushed.

A comparison between the failure pattern of control walls and that of posttensioned walls clearly illustrate that more thin cracks, which are dense and spaced at relative less distance were observed for posttensioned walls. There are fewer cracks in control walls and these inclined cracks are rather wide and in some cases greater than 2 mm. Compared to the replicate posttensioned walls, Yw-a and Yw-b have less damage in the upper walls as shown in Fig. 4g, h. From the test results, it can be concluded that posttensioning and horizontal concrete strip can effectively prevent or mitigate the cracking of the walls.

The failure patterns of the ring beam and constructional columns are illustrated in Fig. 4. No cracks were observed in the ring beam. Several horizontal and diagonal cracks were recorded in the constructional columns. Once the cracks extended throughout the wall and formed X-shape diagonal cracks, the extent of damage extended into the constructional column characterizing by horizontal and diagonal cracks. Furthermore, it was observed that the initiation of cracks in constructional columns depended on the location of the cracks in masonry walls. The first crack formed at the bottom of the columns is diagonal shear crack due to the diagonal strut effect of masonry wall. For most specimens, several flexural cracks were observed in the constructional columns, which is parallel to the direction of loading.

4.2 Test Results

A summary of measured typical test results of each wall is listed in Table 3, where P_C is the initial cracking load and Δ_c is the corresponding displacement, P_u is the shear strength and Δ_f is the corresponding displacement, Δ_u is the ultimate displacement, which is defined as the point at which the lateral wall strength had degraded below 85% of maximum load [19]. σ_p/f_m is the ratio of the axial compression stress provided by PT tendons to the compressive strength of masonry prisms. The ultimate drift capacity is defined as $\gamma_u = \Delta_u/h$. The experimentally determined displacement ductility factor of each wall, which is defined as the ratio of the ultimate displacement to the equivalent yield displacement (i.e., $u = \Delta_u/\Delta_y$) is also summarized in Table 3. The yield displacement was determined using the equivalent energy dissipation capacity approach [20].

With respect to the data in Table 3, the initial cracking load and ultimate shear capacity for posttensioned walls are both considerable higher than those of control walls. The initial cracking load and shear strength of the masonry walls was increased by 48–99%, 65–110%, respectively, with posttensioning, which is attributed to the additional axial compression stress provided by the prestressing force applied to the PT tendons. Generally, unreinforced masonry walls fail in abrupt brittle failure with deforming mainly due to shear under seismic loading, resulting in limited deformation capacity. The cracks and strength of these walls have not been fully developed at the time of brittle failure, resulting in little shear strength. However, the additional axial compressive force provided by posttensioning acts increases the friction in mortar joints, controls crack propagation and encourages a sufficient utilization of the inherent high compressive strength of the masonry, thus enhances the cracking resistance and shear strength of the walls. The posttensioned walls become less brittle and are able to withstand higher tensile and shear stresses. Therefore, it can be concluded that posttensioning can significantly enhance the initial cracking load and ultimate shear capacity of masonry walls.

As shown in Table 3, all specimens had a large ductility factor measured to consistently be above 4.0, which is mainly due to the confinement effect provided by the constructional columns and ring beam. It is, therefore, concluded that the PTCCM walls had considerable inelastic displacement capacity. Furthermore, the ductility factor of posttensioned walls is higher than that of control walls, indicating that posttensioning can improve the deformation capacity of the masonry walls.

A comparison between the initial cracking load and ultimate shear capacity of the walls with opening and without opening clearly illustrates that opening significantly reduced the strength of masonry walls. The initial cracking load and ultimate shear capacity of the masonry walls with horizontal concrete strip are both higher than those of replicate posttensioned walls as shown in Table 3. In addition, the ultimate deformation of these walls is approximately 1.5 times as high as that of replicate posttensioned walls. Therefore, it can be concluded that horizontal concrete strip can effectively enhance the cracking resistance, shear and deformation capacities of masonry walls.

4.3 Force–displacement Hysteretic Response

The lateral load–displacement hysteretic response of each specimen is illustrated in Fig. 5. All walls showed an asymmetric lateral load–displacement response in push and pull directions. Pinching in hysteresis loop for all wall specimens was observed and is more obvious at higher displacement levels. As shown in Fig. 5, a restoring effect was clearly observed for posttensioned walls, which was signified by very stable loops with little residual deformation when the lateral load was removed, namely posttensioned walls return to their original alignment for the majority of the load

Fig. 4 Failure patterns of the specimens **a** W-1; **b** Yw-1; **c** Yw-2; **d** Yw-3; **e** Yw-4; **f** Yw-5; **g** Yw-a; **h** Yw-b; **i** W-a; **j** Yw-c; **k** Yw-d; **l** Dw-1; **m** DYw-1; **n** DYw-2

Table 3 Summary of test results

Specimen	σ_p/f_m	P_C (kN)	Δ_c (mm)	P_u (kN)	Δ_f (mm)	Δ_u (mm)	γ_u (%)	Δ_y (mm)	μ
W-1	0	66.6	0.98	85.0	9.06	10.89	0.605	1.98	5.50
Yw-1	0.133	105.8	1.02	132.2	2.08	8.82	0.490	1.32	6.68
Yw-2	0.165	110.6	0.95	135.5	2.06	7.11	0.395	1.16	6.13
Yw-3	0.151	116.2	1.05	132.6	5.05	8.06	0.448	1.19	6.77
Yw-4	0.175	108.1	1.02	130.2	8.04	13.12	0.729	1.61	8.16
Yw-5	0.067	118.2	1.03	170.6	6.03	12.06	0.670	1.55	7.78
Yw-a	0.064	125.6	0.98	174.6	4.04	15.06	0.837	1.80	8.33
Yw-b	0.078	132.8	0.98	190.4	9.69	15.92	0.884	2.12	7.50
W-a	0	96.9	0.75	130.7	4.02	6.99	0.389	1.33	5.26
Yw-c	0.066	160.8	0.58	227.4	2.93	7.05	0.392	1.07	6.59
Yw-d	0.078	165.4	0.57	224.2	2.86	7.08	0.393	0.93	7.68
Dw-1	0.56	138.3	0.44	234.5	2.34	3.56	0.198	0.81	4.40
DYw-1	0.079	206.7	0.45	338.1	3.90	5.86	0.326	1.19	4.92
DYw-2	0.095	204.5	0.54	325.9	4.16	8.70	0.483	1.63	5.34

history, even after large displacement excursions. This result is consistent with the observation obtained by Laursen and Ingham as well as Rosenboom which indicated that nearly non-linear elastic behavior was observed prior to wall's toe crushing [8, 10].

A comparison of the curves between walls with opening and without opening clearly indicates that walls without opening had considerable higher hysteretic energy dissipation capacity. The area that a hysteretic loop covers of Yw-a and Yw-b with horizontal concrete strip is higher than that of replicate prestressed walls as shown in Fig. 5, which is signified by more slight pinch shape, indicating that the horizontal concrete strip is effective in improving the seismic performance of the walls.

4.4 Overall Force–deformation Response

The force–deformation envelope of each wall is plotted in Fig. 6. The cracking loading points, yield loading points, maximum loading points, and ultimate loading points can be easily recognized as well as the loading process can thus be divided into elastic, elastic–plastic and failure phases. None of these walls exhibited rapid degradation of lateral strength, indicating superior resistance.

A comparison between the shear strength and lateral load degradation rate of control walls and posttensioned walls clearly illustrates the distinct effect of posttensioning. The correlation between the increasing of the shear strength and the increasing prestressing force is clearly shown in Fig. 6. In addition, the effect of opening on shear strength and deformation capacity is readily seen. Figure 6 also clearly reveals the increase of lateral strength from the maximum of 132.2, 135.5 kN for Yw-1, Yw-2 to 174.6, 190.4 KN when horizontal concrete strip was placed beneath the opening in specimens Yw-a and Yw-b, resulting in strength increase of 32.2 and 42.2%, respectively. From test results, it can be concluded that posttensioning and horizontal concrete strip are highly effective in enhancing the shear strength and slowing down the strength degradation of masonry walls.

4.5 Prestressing Force

The strains of PT tendons at different loading stage are summarized in Table 4. For reference, it is noted that the yield strain of PT tendons is about 2350 micro strain. The strains of PT tendons at all loading peaks exceeded the initial strain and increase with the cycling displacement increasing, as shown in Table 4. Recorded data reveals that all PT tendons did not yield and remained elastic stage throughout the loading stage, thus PT tendons retained a significant force and offered a additional compressive force and restoring effect on masonry walls throughout the test, which reduced the residual deformation even after excessive cyclic loading and leaded to an enhancing in shear strength of mortar joints. The test result is consistent with the viewpoint stated by Rosenboom and Kowalsky [10] that the PT tendons should be designed to remain elastic to avoid regions of low stiffness after extensive loading cycles. In this test, determination of the initial stress in PT tendons was based on the assumptions that all tendons should remain elastic at a lateral drift ratio of 1%, thus protecting the PT tendons against inelastic stress.

4.6 Equivalent Viscous Damping

The equivalent viscous damping coefficient ξ_e proposed by Jacobsen is used to represent the energy absorption capacity of masonry walls [21]. The equivalent viscous damping coefficient of each specimen versus the lateral displacements under successive cyclic lateral loads is illustrated in Fig. 7.

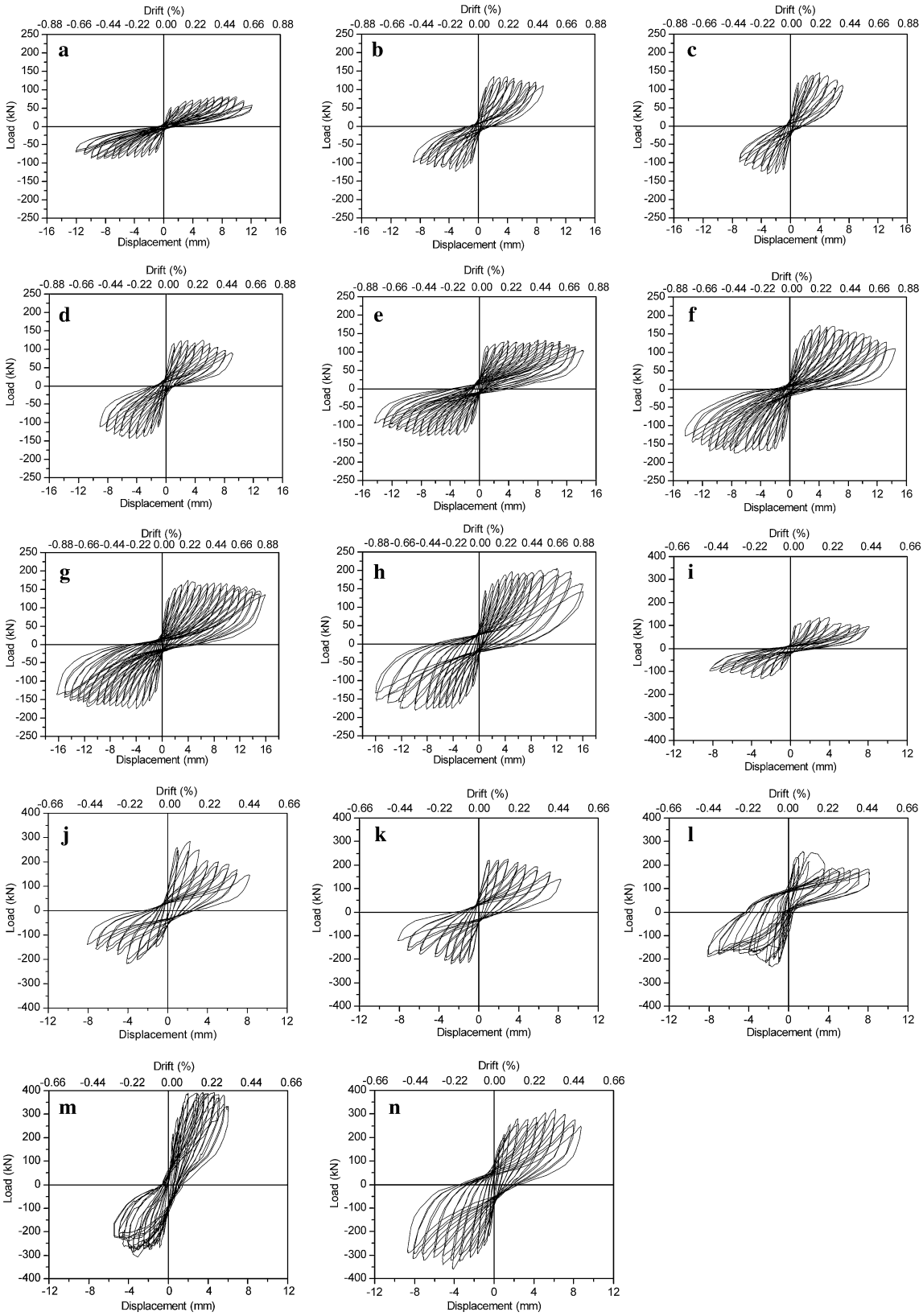

Fig. 5 Load–displacement hysteretic response **a** W-1; **b** Yw-1; **c** Yw-2; **d** Yw-3; **e** Yw-4; **f** Yw-5; **g** Yw-a; **h** Yw-b; **i** W-a; **j** Yw-c; **k** Yw-d; **l** Dw-1; **m** DYw-1; **n** DYw-2

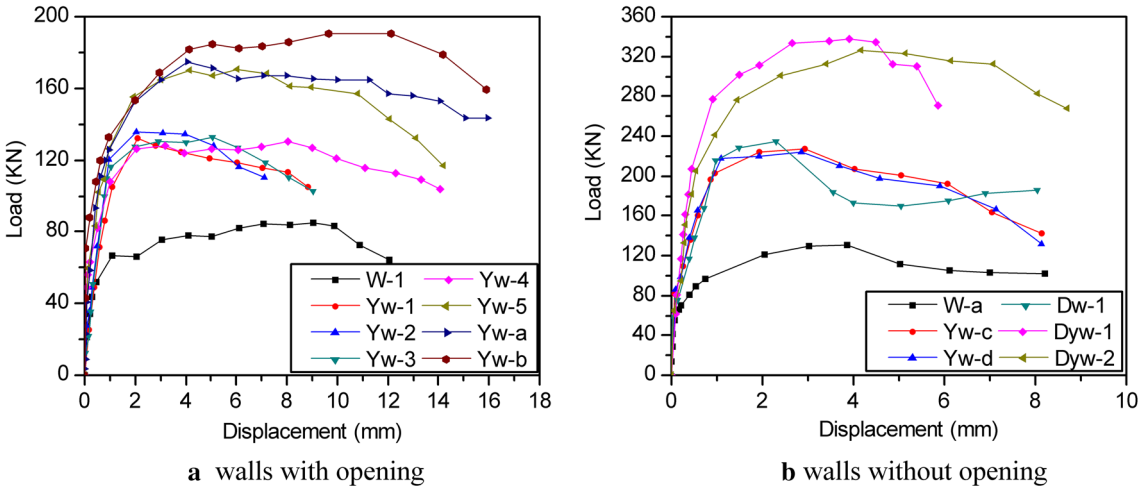

Fig. 6 Load–displacement envelope **a** walls with opening; **b** walls without opening

As can be seen from Fig. 7, the equivalent viscous damping coefficient of posttensioned walls is higher than that of control wall. The equivalent viscous damping coefficient of posttensioned walls with horizontal concrete strip is higher than that of replicate posttensioned walls. From test results, it can be concluded that posttensioning and horizontal concrete strip can enhance the energy dissipation capacity of masonry walls, which is due to the reason that cracks closed again under the posttensioning acts when lateral loads were removed, and each cycle of the opening and closure of cracks can dissipate considerable seismic energy, thus successfully improves the energy dissipation capacity of masonry walls. Furthermore, the integrity of the masonry walls is also strengthened with posttensioning.

Table 4 Strains of the posttensioned (PT) tendons

Specimen	$\varepsilon_i(\mu\varepsilon)$	$\varepsilon_c(\mu\varepsilon)$	$\varepsilon_f(\mu\varepsilon)$	$\varepsilon_u(\mu\varepsilon)$
Yw-1	899	926	1276	1639
Yw-2	820	862	1127	1939
sYw-3	1094	1155	1769	2116
Yw-4	834	902	1066	1765
Yw-5	898	914	1109	1576
Yw-a	859	940	1124	1576
Yw-b	1058	1141	1553	1715
Yw-c	831	1018	1313	1550
Yw-d	1189	1381	1712	1927
DYw-1	1061	1224	1445	1649
DYw-2	907	1040	1213	1566

ε_i is the initial strain; ε_c is the strain when first crack was observed; ε_f is the strain corresponding to maximum lateral load; ε_u is the strain at extreme displacement

As shown in Fig. 7, the equivalent viscous damping value of PTCCM walls is about 10%, which is similar to that of PTCM walls proposed by Rosenboom and Kowalsky [10, 22], in which an equivalent viscous damping value of about 12% was measured. According to the test results, a damping value of 5% for ungrouted PTCCM walls would be reasonable for seismic design.

4.7 Stiffness Degradation

The secant stiffness degradation curve of each wall against the increase of drift ratio is plotted in Fig. 8. When cracks were observed in the walls, the secant stiffness decreased dramatically (i.e. less than 60% of its initial stiffness). At the later stage of loading, the stiffness degeneration of all walls tended to be slow and the decreasing rate was relieved. Figure 8 also presents the comparisons of the stiffness and stiffness degradation between all wall specimens. The stiffness is commonly higher and degenerated slower in posttensioned walls than in control walls, indicating that posttensioning can enhance the stiffness and slow down the stiffness degradation of masonry walls, which is attributed to the additional axial compressive force restricted the lateral movement of the walls. In addition, the stiffness of the walls without opening is generally higher than that of the walls with opening, indicating that opening looses the lateral movement of walls. A comparison between posttensioned walls with horizontal concrete strip and replicate posttensioned walls clearly reveals that horizontal concrete strip can increase the stiffness and slow down the stiffness degradation of masonry walls.

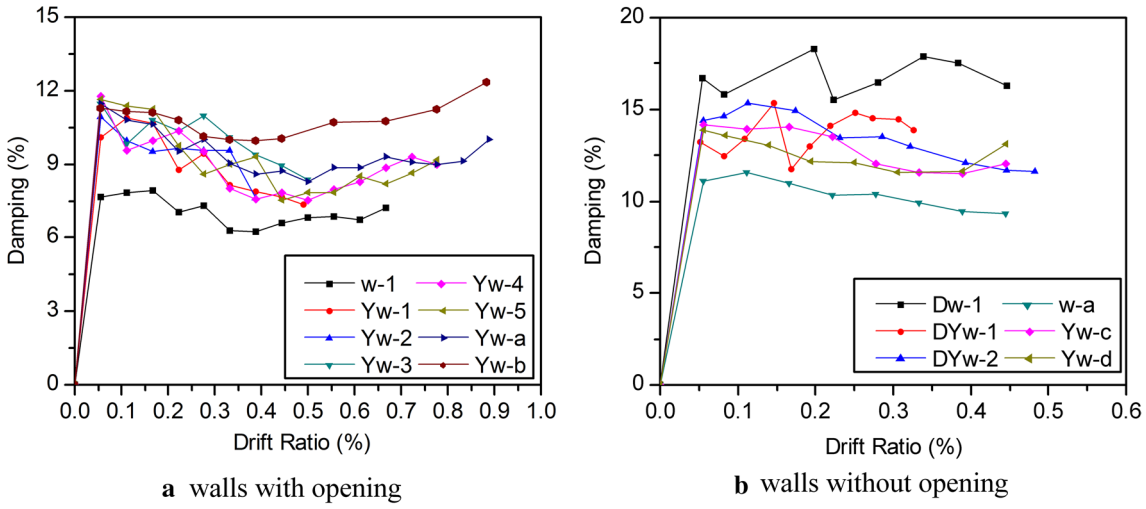

Fig. 7 Equivalent viscous damping coefficient **a** walls with opening; **b** walls without opening

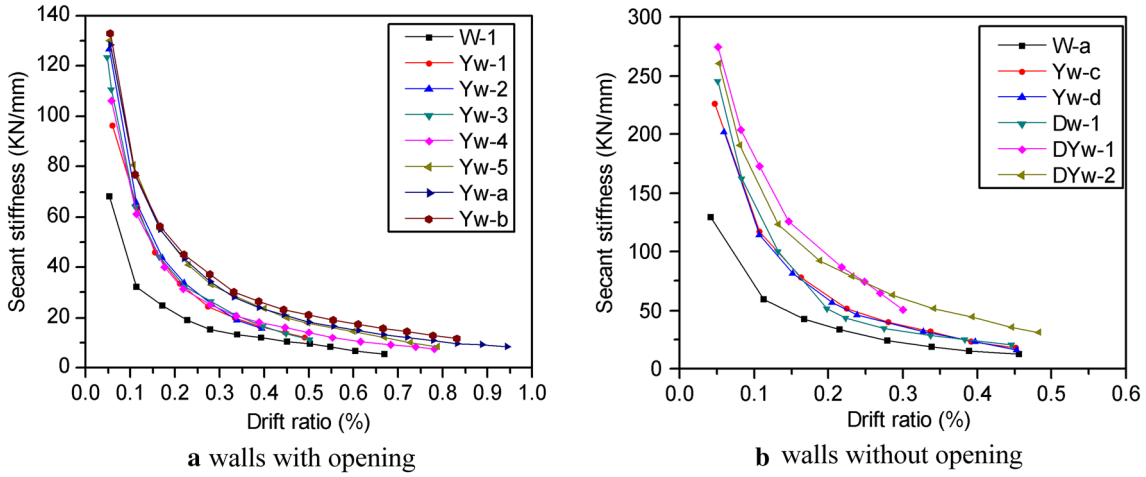

Fig. 8 Stiffness degradation against drift ratio **a** walls with opening; **b** walls without opening

5 Prediction of Shear Capacity

The shear force applied to a PTCCM walls is assumed to be resisted by masonry wall and constructional columns. Hence, the ultimate shear capacity V_u of PTCCM walls can be calculated using the following equation:

$$V_u = V_m + V_c \tag{1}$$

where V_m and V_c is the shear capacity provided by masonry wall and constructional columns, respectively. Test results indicate that posttensioning can significantly enhance the shear strength of the walls, which is due to the additional vertical compression stress σ_p provided by posttensioning. Furthermore, according to the test results, PT tendons elongated greatly during the cyclic lateral loading process, resulting in an increase in the ultimate capacity of the walls, which is consistent with the conclusion proposed by Hassanli [13] and Dongun [23]. In this research, the role of PT tendons elongation in increasing shear capacity is considered as an effective coefficient ζ_p. Gavin [24] and Hassanli [14, 25] found that σ_p/f_m is the most important factor in determining elongation magnitudes in PT tendons and the elongation magnitudes decreased with the ratio of σ_p/f_m increasing. Thus, ζ_p can be calculated as follows:

$$\zeta_p = 1 + \alpha\frac{f_m}{\sigma_p} \tag{2}$$

where α is the regression factor. Therefore, the shear capacity of masonry walls can be calculated in the following form:

$$V_m = \zeta_p f_v A_m \tag{3}$$

where A_m is the cross-section area of the walls, f_v is the shear strength of masonry walls and can be calculated using following Eq. [15]:

$$f_v = f_{vo} + \mu_o \sigma_y \tag{4}$$

where f_{vo} is the shear strength of masonry in the absence of vertical compression stress. μ_o is the friction coefficient and a value of 0.4 is adopted according to Chinese code (GB50003-2011) [15]. σ_y is the total axial compression stress of the walls, including the additional vertical stress provided by posttensioning.

The shear force resisted by constructional columns V_c is complex and still controversial, because the mechanism is significantly dependent on the distance between constructional columns and the aspect ratio of masonry walls. The shear force applied to a reinforced concrete column is assumed to be resisted by concrete and transverse stirrups. Yang JJ et al. [26] conducted a series of research to study the strength of masonry walls with constructional columns and found that constructional columns are commonly insufficient developed. According to the test results, a reduction coefficient ζ_g with a value of 0.28 was proposed by Yang JJ et al. to consider the limited efficiency of the shear strength of constructional columns. Therefore, the shear capacity provided by constructional column V_c can be calculated using the following equation:

$$\begin{aligned} V_c &= \zeta_g \left(0.07 f_{cu} A_c + 1.25 f_{yv} \frac{A_{sv}}{s} h_0 \right) \\ &= 0.28 \left(0.07 f_{cu} A_c + 1.25 f_{yv} \frac{A_{sv}}{s} h_0 \right), \end{aligned} \tag{5}$$

where f_{cu} is the cubic compressive strength of concrete, f_{yv} is the yield strength of stirrups, A_{sv} and s is the cross-section area and distance of stirrups, respectively, A_c and h_0 is the cross-section area and effective length of constructional columns, respectively.

Nonlinear regression analysis using test results was carried out to reasonably assess the shear strength of PTCCM walls. The regression factor α was considered as the main parameter affecting the shear capacity of the walls and a value of 0.01 was obtained by the regression of test results. Therefore, the shear capacity of PTCCM walls can be calculated as follows:

$$V_u = \left(1 + 0.01 \frac{f_m}{\sigma_p} \right) f_v A_m + 0.28 \left(0.07 f_{cu} A_c + 1.25 f_{yv} \frac{A_{sv}}{s} h_o \right). \tag{6}$$

Table 5 shows the shear strength predictions for the walls according to Eq. (6) and the comparisons with test results. It is clear that there is a close agreement between the predictions and test results. The ultimate shear strength predicted from Eq. (6) is slightly less than the test results.

Table 5 Comparison of predictions and test results

Specimen	σ_p/f_m	Test results P_u (kN)	Calculated results V_u (kN)	V_u/P_u
W-1	0	85.00	80.64	0.95
Yw-1	0.133	132.20	133.05	1.01
Yw-2	0.165	135.50	143.47	1.06
Yw-3	0.151	132.60	138.81	1.05
Yw-4	0.175	130.20	146.98	1.13
Yw-5	0.067	170.60	160.73	0.94
Yw-a	0.064	174.60	158.5	0.91
Yw-b	0.078	190.39	167.35	0.88
W-a	0	130.70	123.01	0.94
Yw-c	0.066	227.40	217.13	0.95
Yw-d	0.078	224.20	228.6	1.02
DW-1	0	234.50	195.23	0.83
DYw-1	0.079	333.46	286.16	0.86
DYw-2	0.095	325.90	299.76	0.92

The average value and standard deviation of the ratios between test results and predictions is 0.96 and 0.03, respectively.

6 Conclusions

This paper presents an experimental study on the seismic performance of the PTCCM walls. A simple analytical approach for predicting the shear strength of PTCCM walls is proposed. The experimental results and theoretical analysis stated in this study allow the following conclusions to be drawn:

1. Under cyclic lateral loads, the PTCCM walls performed in a similar behavior and failed in a shear failure mode, signified by X-shape diagonal cracks extending throughout the walls.
2. Posttensioning and constructional columns as well as ring beam are significantly effective in improving the structural performance of the walls. The seismic behavior of PTCCM walls is similar to that of PTCM walls, but the construction process is simpler and the cost is declined. Thus, PTCCM wall is a competent, effective, and economical structural wall system for low-rise buildings.
3. Opening reduce the cracking resistance and shear strength of the walls. Horizontal concrete strip placed below the opening can significantly enhance the shear and deformation capacity of masonry walls. Further improvement may be developed if the cells on both sides of opening are grouted or structural columns are placed

on both sides of opening, but further work is needed to validate the effectiveness of this configuration technique.
4. The presented approach, using an effective coefficient to consider the contribution of PT tendons elongation, can accurately to predict the shear strength of PTCCM walls.

Acknowledgements The research described here was supported by National Natural Science Foundation of China (Grant No. 50708045). The experiments were conducted at the Jiangsu Key Laboratory of Civil Engineering and Disaster Prevention and Mitigation. The authors wish to gratefully acknowledge the support of these organizations for this study.

References

1. Sun WM, Ye YH, Guo ZG, Li LQ (2007) Experimental study on seismic behavior of prestressed masonry constructed by hollow concrete blocks. In: proceeding of 2007 ANCER meeting, Hong-Kong, May 29–30
2. Zhao B, Taucer F, Rossetto T (2009) Field investigation on the performance of building structures during the 12 May 2008 Wenchuan earthquake in China. Eng Struct 31(8):1707–1723
3. Eshghi S, Pourazin K (2009) In-plane behavior of confined masonry walls with and without opening. Int J Civ Eng 7(1):49–60
4. Choi H-K, Bae B-I, Choi C-S (2016) Lateral strength of unreinforced masonry walls strengthened with engineered cementitious composite. Int J Civ Eng 14(6):411–424
5. Ma RL, Jiang L (2012) Experimental investigations on masonry structures using external prestressing techniques for improving seismic performance. Eng Struct 42:297–307
6. Shultz AE, Scolforo MJ (1999) An overview of prestressed masonry. Mason Soc J 10(1):6–21
7. Laursen PT, Ingham JM (2004) Structural testing of enhanced posttensioned concrete masonry walls. ACI Struct J 101(6):852–862
8. Laursen PT, Ingham JM (2004) Structural testing of large-scale posttensioned concrete masonry walls. J Struct Eng 130(10):1497–1505
9. Laursen PT, Ingham JM (2001) Structural testing of single-storey posttensioned concrete masonry walls. TMS J 19(1):69–82
10. Rosenboom OA, Kowalsky MJ (2004) Reversed in-plane cyclic behavior of posttensioned clay brick masonry walls. J Struct Eng 130(5):787–798
11. Wight GD, Kowalsky MJ, Ingham JM (2007) Shake table testing of posttensioned concrete masonry walls with openings. J Struct Eng 133(11):1551–1560
12. Wight GD, Ingham JM, Wilton AR (2007) Innovative seismic design of a posttensioned concrete masonry house. Can J Civ Eng 34(11):1393–1402
13. Hassanli R, El Gawady A, Mills JE (2016) Experimental investigation of in-plane cyclic response of unbonded posttensioned masonry walls. J Struct Eng ASCE 2016 142(5):04015171
14. Hassanli R, El Gawady MA, Mills J (2017) In-plane flexural strength of unbonded posttensioned concrete masonry walls. Eng Struct 136:245–260
15. China Ministry of Construction (2011) Code for design of masonry structures (GB50003–2011). China Architecture & Building Press, Beijing
16. China Ministry of Construction (2002) Test method of mechanical properties on ordinary concrete (GB/T 50081-2002). China Architecture & Building Press, Beijing
17. China Ministry of Construction (2011) Test method standards for basic mechanical properties of masonry (GB/T50129-2011). China Architecture & Building Press, Beijing
18. China Ministry of Construction (2010) Metallic materials tensile testing at ambient temperature (GB/T228.1-2010). China Architecture & Building Press, Beijing
19. China Ministry of Construction (1997). Specification for seismic test of buildings (JGJ101–1996). China Architecture & Building Press, Beijing
20. Park R (1989) Evaluation of ductility of structures and structural assemblages from laboratory testing. Bull NZ Soc Earthq Eng 22(3):155–166
21. Jacobsen LS (1930) Steady forced vibrations as influenced by damping. ASME Trans 52(1):169–181
22. Rosenboom OA (2002) Post-tensioned clay brick masonry walls for modular housing in seismic regions. M.S. thesis, North Carolina State Univ., Raleigh, NC
23. Dongun R, Anil C, Mohamed AE (2014) Effects of tendon spacing on in-plane behavior of posttensioned masonry walls. J Struct Eng 140(4):04013096 **(1–04013096–13)**
24. Wight GD, Ingham JM (2008) Tendon stress in unbonded posttensioned masonry walls at nominal in-plane strength. J Struct Eng 134(6):938–946
25. Hassanli R, El Gawady MA, Mills J (2015) Strength and seismic performance factors of posttensioned masonry walls. J Struct Eng 141(11):04015038 **(1–04015038–15)**
26. Yang JJ, Gao YF, Zhao D (1998) Shear strength analysis of concrete block masonry coupled with constructural columns and ring beam. J Build Struct 19(3):64–70 **(Chinese)**